

doi: 10.1002/adma.((please add manuscript number))

Dynamically Doped White Light Emitting Tandem Devices

Takeo Akatsuka, Cristina Roldán-Carmona, Enrique Ortí, and Henk J. Bolink*

Lighting accounts for about 10% of the world global energy consumption. There is therefore a strong incentive for new, low-consumption lighting solutions to reduce global energy demand. In this context, organic light-emitting diodes (OLEDs) have considerable advantages compared to other solid-state lighting technologies, which are based on inorganic semiconductors.^[1] Currently, best-performing white OLEDs are based on a tandem approach, in which two or more sub-devices are stacked on top of each other.^[2] In tandem OLEDs the middle electrode needs to inject electrons and holes in the adjacent sub-devices, which is an energetically unfavorable process when air-stable metals are used as the middle contact.^[3] For this reason, doped layers are used adjacent to or as the middle contact to facilitate electron and hole injection into the sub-devices.^[4] As it is very difficult to prepare doped injection layers using solution-based processes, almost all tandem OLEDs are prepared using high-vacuum sublimation of the active materials. Only one example of a solution-processed tandem OLED has been reported, in which a Cs₂CO₃/ZnO n-doped electron injection layer was processed from solution by blending it with poly(4-vinylpyridine).^[5] The infrastructure investment for multiple vacuum sublimation tools, especially for large areas, is elevated, making the production of low-cost OLEDs only possible if very high production volumes are reached.

Mr. T. Akatsuka, Mrs. C. Roldán-Carmona, Prof. E. Ortí and Dr. H. J. Bolink
Instituto de Ciencia Molecular, Universidad de Valencia, C/ Catedrático J. Beltrán 2, 46980 Paterna (Valencia), Spain
Email: henk.bolink@uv.es

Mr. T. Akatsuka
Nippon Shokubai Co., Ltd. 5-8 Nishi Otabi-cho, Suita 564-8512 Osaka, Japan.

Mrs. C. Roldán-Carmona
Department of Physical Chemistry and Applied Thermodynamics, University of Cordoba, Campus de Rabanales,
Edificio Marie Curie, 14014 Córdoba, Spain

Solution-based processing requires lower investments and is compatible with high throughput, hence this technique is more suitable for low-cost device production. Another type of electroluminescent device, referred to as light-emitting electrochemical cell (LEC), contain salts in the light-emitting layer and have a much simpler architecture.^[6] Contrary to OLEDs,^[4a] LECs do not rely on air-sensitive injection layers and metals used for electron injection.^[6a, 7] This facilitates solution processing and reduces the encapsulation requirements^[8] LECs are based on either a conjugated light-emitting polymer mixed with a salt^[7c] or an ionic transition-metal complex (iTMC).^[7d] Recently, it was shown that both types of LECs operate according the same mechanism governed principally by the ionic conductivity of the salts in the thin film.^[9]

The operating mechanism of LECs involves the dissociation of the salt in the active layer and, subsequently, the migration of the constituent ions towards the electrode interfaces leading to the formation of doped zones [Figure 1, panel (a) and (b)].^[10] In a tandem LEC, such dynamically doped layers will be generated on both sides of the middle electrode removing the injection barriers for electrons and holes and allowing for efficient electroluminescence [Figure 1, panel (c) and (d)]. Therefore, no intentionally doped layers are required adjacent to the middle electrode, which facilitates the solution processing of tandem light-emitting devices. A first hint that it should be possible to prepare tandem LECs in this way was obtained from the report of cascaded LECs, in which the electrodes are used simultaneously as anode and cathode for laterally connected cells.^[11]

White LECs based on both polymer- and iTMC-emitting materials have been reported using different methods such as blending two or three emitters,^[12] profiting from dual emission from a single polymer,^[13] and employing a color conversion layer.^[14] However, these devices only work efficiently at low luminance values. The main reason for the poor performance of white LECs is the lack of a good blue light-emitting device. In blue light-emitting iTMC-based LECs, efficiencies up to 18.3 cd A⁻¹ have been reported, but only at low current densities and, consequently, at low luminances (14.5 cd m⁻²).^[12b] In tandem devices both sub-devices operate with the same current

density. Therefore, if the before-mentioned blue LECs are used to prepare tandem LECs, their maximum luminance would be severely limited. Hence, to confirm that indeed LECs are ideally suited for solution-processed tandem devices, a better blue LEC is required that can function as the blue-emitting sub-device. Orange LECs with high luminance and efficiency, on the contrary, are quite abundant.

Here we report white light-emitting LECs, based on a tandem structure and employing an air stable middle electrode, that exhibit a current efficiency of 8.4 cd A^{-1} at a luminance of 845 cd m^{-2} . The tandem LEC consists of a novel polymer-composite as the bottom blue light-emitting layer and an ionic iridium complex as the top orange light-emitting layer, both prepared using solution processing.

In view of the limited luminance and efficiency of iTMC-based blue LECs, we developed an alternative based on a well-known blue light-emitting OLED configuration. In this configuration, the neutral hole transporting host poly(N-vinylcarbazol) (PVK), the neutral electron transporter 1,3-bis[2-(4-*tert*-butylphenyl)-1,3,4-oxadiazol-5-yl]benzene (OXD-7), and the blue emitter bis[2-(4',6'-difluoro-phenyl)pyridinato-N,C2']iridium(III)-picolinate (FIrPic) were mixed with a small amount of the ionic liquid (IL) tetrahexylammonium tetrafluoroborate [THA][BF₄] (**Figure 2** panel a). A similar approach for red LECs was reported by Shin et al.^[15] The device had the following configuration: ITO/PEDOT:PSS/PVK:OXD-7:FIrPic:IL=10:10:2:1 (mass ratio)/Au (Figure 2, panel a and c) and reached a maximum luminance of 160 cd m^{-2} at a constant current of 100 A m^{-2} (see **Figure 3**, panel a). When an aluminum cathode was used, the performance of this blue LEC improved to a luminance of 400 cd m^{-2} (8.4 cd A^{-1}) (Figure S1 in the Supporting Information).

To identify a complementary broad-band orange light-emitter, the electroluminescence spectrum of the FIrPic-based bottom LEC (**Figure 3**, panel b) was compared with that of many different orange LECs. This was done screening the literature as well as our own database. From

this comparison, a rather good match was found for the orange LEC using the iTMC [Ir(ppy)₂(dtb-bpy)][PF₆], where Hppy stands for 2-phenylpyridine and dtb-bpy for 4,4'-di-*tert*-butyl-2,2'-bipyridine, as the emitter (Figure 3, panel b).^[16] Hence, the top LEC was prepared using this emitter, mixed with the IL 1-butyl-3-methylimidazolium hexafluorophosphate [BMIm][PF₆], and Au as the semi-transparent anode. A thin layer of Cr was used to ensure good adhesion of the semitransparent gold electrode on the glass substrate. To maintain a good transparency, the bottom electrode was built up using 2 nm of Cr, 5 nm of Au and 5 nm of MoO₃ (the reason for the MoO₃ layer is commented upon in the next paragraph), deposited by sequential thermal vacuum evaporation on top of a flat glass substrate (Figure 2, panel d). The maximum luminance of the Cr/Au/MoO₃/iTMC:[BMIm][PF₆]=4:1 (molar ratio)/Al top LEC reaches 727 cd m⁻² at a constant current of 100 A m⁻² (see Figure 3, panel a).

In addition to the charge generation function, the middle electrode has the role of protecting the bottom device during the processing of the top device. In this work Au layers of 0, 5, 10, and 40 nm were evaluated as the semitransparent middle electrode. With thin Au layers, the bottom device was partially removed during the solution processing of the top light-emitting layer. Hence, an additional layer is required to prevent damaging of the bottom device. In tandem OLEDs using doped electron injection layers, MoO₃ has been used as the interlayer.^[2f] Therefore, a thin layer of MoO₃ was thermally evaporated on top of the Au electrode in the tandem LECs. A MoO₃ layer as thin as 5 nm on top of the Au electrode is sufficient to protect the bottom layer during processing of the top device.

To verify the effect of the different Au thicknesses, the electrodes used in the tandem device had a different area, 78, 72, and 36 mm² for the ITO bottom-, the Au middle-, and the Al top-electrode, respectively (Figure 3, panel c). The tandem LEC without Au did emit but the light was orange indicating it came from the top device only. Hence, in contrast to what was observed in a tandem OLED, no electron injection into the bottom device is occurring from the MoO₃ layer. This

suggests that the dynamic doping levels in LECs are lower than what is achieved by intentionally doping. The tandem device with a very thick Au layer (40 nm) had a very poor transparency and, although both sub-devices emit light, only very weak orange light is detected from the top device. The tandem LEC with 10 nm Au emits from both top and bottom devices leading to white light emission (Figure 3, panel d). Additionally, blue light emission is obtained over the area where the Au electrode overlaps with the ITO anode. Hence, electrons are injected into the bottom device over the whole area of the Au middle electrode, implying that its lateral conductivity is higher than required. At the area at which there is no overlap between the Al cathode and the ITO anode but with the Au interlayer present, only orange light from the top device is observed (Figure 3, panel d). This demonstrates nicely the tandem device concept showing simultaneously light-emission from bottom, top and tandem device. The best tandem LEC was obtained with a Au layer of 5 nm. In this tandem device, light emission (white) is only observed from the area at which the Al cathode overlaps with the ITO anode (Figure 3, panel e). Now, the lateral conductivity of the thin Au layer is insufficient to allow for the injection of electrons outside the area defined by the top contact. For this reason, no light-emission can be observed for the bottom and top cell separately.

The typical performance of the optimized tandem LEC is depicted in Figure 3 (panels a and b). The electroluminescence of the tandem LEC clearly contains contributions from bottom and top devices (Figure 3, panel b). The CIE coordinates of the white light emitted are $x = 0.38$ and $y = 0.47$, which is slightly above the black-body radiation curve. The driving voltage of the tandem LEC drops rapidly after turning-on the current (Figure 3, panel a). The drop is caused by the migration of ions to the electrode interfaces and the build-up of electrical double layers and, eventually, the formation of the dynamically doped zones, which rapidly reduces the injection barriers for electrons and holes (Figure 1). As such, the voltage needed to sustain a current density of 100 A m^{-2} continuously decreases until it reaches a quasi-steady-state, which is related to the charge transport of the carriers in the light-emitting layers. The luminescence of the white tandem LEC reaches a

maximum of 845 cd m^{-2} at a constant current of 100 A m^{-2} . At this luminance the current efficiency is 8.45 cd A^{-1} (**Table 1**). Although device performance was not the main goal of this work, these values are significantly above those reported previously for white LECs.^[12-14] The luminance of the tandem LEC decreases quite rapidly with time mainly due to the poor stability of the bottom blue LEC.

For a tandem configuration with two devices in series, the luminance and the driving voltage are expected to be the sum of the two individual devices. Interestingly, the tandem LEC here described shows a higher luminance and a lower driving voltage than what is obtained from the sum of luminance and driving voltage performance values for the bottom and top LEC separately (Figure 3, panel a). This observation implies that the individual cells in the tandem configuration outperform the stand alone bottom and top LECs. Moreover, there appears to be no charge balancing issue with this tandem device. That is expected as the formation of the dynamic doped zones is a self-regulating mechanism causing the current density to be equal in both top and bottom devices without potential losses at the junction.

In summary, salt-containing organic semiconducting materials are ideally suited for the preparation of tandem devices. Upon applying an external bias, the presence of the ions lead to the generation of dynamically doped regions adjacent to the external and internal electrodes. This self-regulates the potential drop, leads to ideal junction formation, and removes the need to use permanently doped charge injection layers. This was demonstrated by preparing a partially solution-processed white tandem LEC exhibiting a current efficiency of 8.4 cd A^{-1} at a luminance of 845 cd m^{-2} . To achieve this, a novel high-luminance blue LEC was developed by adding an ionic liquid to a composite frequently employed in OLEDs

Experimental Section

Materials: Aqueous dispersions of poly(3,4-ethylenedioxythiophene) doped with poly(styrenesulfonate) (PEDOT:PSS, CLEVIOS P VP Al 4083) were obtained from Heraeus Holding GmbH and used as received. The ionic transition-metal complex (iTMC) 4,4'-di(*tert*-butyl)-2,2'-bipyridine bis(2-phenylpyridinato) iridium(III) hexafluorophosphate [Ir(ppy)₂(dtb-bpy)][PF₆] was synthesized following a previously published procedure.^[16] The ionic liquids (ILs) 1-butyl-3-methyl-imidazolium hexafluorophosphate [BMIm][PF₆] and tetrahexylammonium tetrafluoroborate [THA][BF₄] were purchased from Aldrich and Fluka, respectively. The host-polymer poly(N-vinylcarbazol) (PVK) was purchased from Aldrich and 1,3-bis[2-(4-*tert*-butylphenyl)-1,3,4-oxadiazol-5-yl]benzene (OXD-7) was purchased from Luminescence Technology Corp. The phosphorescent guest bis(2-(4',6'-difluoro)phenylpyridinato)iridium(III) picolinate (FIrPic) was also purchased from Luminescence Technology Corp. All commercially available materials were used as received. The chemical structure of the iTMC, the ILs, and the phosphorescent host-guest materials are displayed in Figure 2.

Device preparation: The tandem LECs were made as follows. Indium tin oxide ITO-coated glass plates were patterned by conventional photolithography (purchased from Naranjo substrates). The substrates were subsequently cleaned ultrasonically in water-soap, water, and 2-propanol baths. After drying, the substrates were placed in a UV-ozone cleaner (Jelight 42-220) for 20 min. An 80 nm layer of PEDOT:PSS was spin-coated on the ITO glass substrate. A first emitting layer of FIrPic in a composite matrix, comprising 10 mg of PVK, 10 mg of OXD-7, 2 mg of FIrPic, and 1 mg of [THA][BF₄] in 10 mL chlorobenzene, was spin-coated at 1500 rpm for 40 s on top of the PEDOT:PSS layer. Then the gold and the molybdenum oxide (5 nm) as the middle electrode were thermally evaporated using a shadow mask. After that, a second light-emitting layer consisting of the iTMC and [BMIm][PF₆] at a molar ratio of 4 to 1 was spin-coated from an acetonitrile solution (solid content 40 mg mL⁻¹) at 1500 rpm for 40 s on top of the middle electrode layer. Finally the

top Al electrode (70 nm) was thermally evaporated. Spin-coating was done in ambient atmosphere; the base pressure during the thermal evaporation was 1×10^{-6} mbar.

Device Characterization: The thickness of the films was determined with an Ambios XP-1 profilometer. Thin film photoluminescence spectra and quantum yields were measured with a Hamamatsu C9920-02 Absolute PL Quantum Yield Measurement System. The current-density versus voltage (J - V) and electroluminescence versus voltage (Lum - V) characteristics were collected using a Keithley Model 2400 source measurement unit and a Si-photodiode coupled to a Keithley Model 6485 picoamperometer, respectively. The photocurrent was calibrated using a Minolta Model LS100 luminance meter. Electroluminescence spectra were recorded using an Avantis fiberoptics photospectrometer. The devices were not encapsulated and were characterized inside the glovebox.

Supporting Information

Supplementary information showing performance data of the blue bottom LEC.

Acknowledgements

We are grateful to Edwin Constable and Catherine Housecroft of the University of Basel for supply of the Iridium complex. This work has been supported by the European Union (CELLO, Grant STRP 248043; <https://www.cello-project.eu/>), the Spanish Ministry of Economy and Competitiveness (MINECO) (MAT2011-24594 and CTQ2012-31914), the Generalitat Valenciana (Prometeo/2012/053), and European FEDER funds (CTQ2012-31914). C.R. would like to thank the MINECO for the financial support of this research in the framework of project CTQ2010-17481, the Junta de Andalucía (CICyE) for special financial support (P08-FQM-4011 and P10-FQM-6703) and the MECD (Spanish Ministry of Education, Culture, and Sport) for an FPU grant.

References

- [1] aJ. H. Burroughes, D. D. C. Bradley, A. R. Brown, R. N. Marks, K. Mackay, R. H. Friend, P. L. Burns, A. B. Holmes, *Nature* **1990**, 347, 539-541; bC. W. Tang, S. A. VanSlyke, *Appl. Phys. Lett.* **1987**, 51, 913-915.
- [2] aJ. Kido, M. Kimura, K. Nagai, *Science* **1995**, 267, 1332-1334; bS. Reineke, F. Lindner, G. Schwartz, N. Seidler, K. Walzer, B. Lussem, K. Leo, *Nature* **2009**, 459, 234-U116; cT. Chiba, Y.-J. Pu, R. Miyazaki, K.-i. Nakayama, H. Sasabe, J. Kido, *Org. Electron.* **2011**, 12, 710-715; dM. C. Gather, A. Köhnen, K. Meerholz, *Adv. Mater.* **2011**, 23, 233-248; eT. Matsumoto, T. Nakada, J. Endo, K. Mori, N. Kawamura, A. Yokoi, J. Kido, *Dig. Tech. Pap. - Soc. Inf. Disp. Int. Symp.* **2003**, 34, 979; fH. Kanno, R. J. Holmes, Y. Sun, S. Kena-Cohen, S. R. Forrest, *Adv. Mater.* **2006**, 18, 339-342.
- [3] aS. Hamwi, J. Meyer, M. Kröger, T. Winkler, M. Witte, T. Riedl, A. Kahn, W. Kowalsky, *Adv. Funct. Mater.* **2010**, 20, 1762-1766; bQ.-Y. Bao, J.-P. Yang, J.-X. Tang, Y. Li, C.-S. Lee, S.-T. Lee, *Org. Electron.* **2010**, 11, 1578-1583.
- [4] aK. Walzer, B. Maennig, M. Pfeiffer, K. Leo, *Chem. Rev.* **2007**, 107, 1233-1271; bY. Chen, D. Ma, *J. Mater. Chem.* **2012**, 22, 18718-18734.
- [5] T. Chiba, Y.-J. Pu, H. Sasabe, J. Kido, Y. Yang, *J. Mater. Chem.* **2012**, 22, 22769-22773.
- [6] aQ. B. Pei, G. Yu, C. Zhang, Y. Yang, A. J. Heeger, *Science* **1995**, 269, 1086-1088; bJ.-K. Lee, D. S. Yoo, E. S. Handy, M. F. Rubner, *Appl. Phys. Lett.* **1996**, 69, 1686-1688.
- [7] aK. M. Maness, R. H. Terrill, T. J. Meyer, R. W. Murray, R. M. Wightman, *J. Am. Chem. Soc.* **1996**, 118, 10609-10616; bJ. D. Slinker, J. Rivnay, J. S. Moskowitz, J. B. Parker, S. Bernhard, H. D. Abruna, G. G. Malliaras, *J. Mater. Chem.* **2007**, 17, 2976-2988; cQ. J. Sun, Y. F. Li, Q. B. Pei, *J. Display Technol.* **2007**, 3, 211-224; dR. D. Costa, E. Ortí, H. J. Bolink, F. Monti, G. Accorsi, N. Armadori, *Angew. Chem. Int. Ed.* **2012**, 51, 8178-8211; eT. Hu, L. He, L. Duan, Y. Qiu, *J. Mater. Chem.* **2012**, 22, 4206-4215.
- [8] A. Sandström, H. F. Dam, F. C. Krebs, L. Edman, *Nat. Commun.* **2012**, 3, 1002.
- [9] S. van Reenen, T. Akatsuka, D. Tordera, M. Kemerink, H. J. Bolink, *J. Am. Chem. Soc.* **2013**, 135, 886-891.
- [10] aP. Matyba, K. Maturova, M. Kemerink, N. D. Robinson, L. Edman, *Nature Mater.* **2009**, 8, 672-676; bS. van Reenen, P. Matyba, A. Dzwilewski, R. A. J. Janssen, L. Edman, M. Kemerink, *J. Am. Chem. Soc.* **2010**, 132, 13776-13781; cM. Lenes, G. García-Belmonte, D. Tordera, A. Pertegás, J. Bisquert, H. J. Bolink, *Adv. Funct. Mater.* **2011**, 21, 1581-1586.
- [11] aC. Tracy, J. Gao, *Appl. Phys. Lett.* **2005**, 87, 143502; bJ. D. Slinker, J. Rivnay, J. A. DeFranco, D. A. Bernards, A. A. Gorodetsky, S. T. Parker, M. P. Cox, R. Rohl, G. G. Malliaras, S. Flores-Torres, H. D. Abruna, *J. Appl. Phys.* **2006**, 99.
- [12] aL. He, J. Qiao, L. Duan, G. F. Dong, D. Q. Zhang, L. D. Wang, Y. Qiu, *Adv. Funct. Mater.* **2009**, 19, 2950-2960; bL. He, L. A. Duan, J. A. Qiao, G. F. Dong, L. D. Wang, Y. Qiu, *Chem. Mater.* **2010**, 22, 3535-3542; cH. C. Su, H. F. Chen, Y. C. Shen, C. T. Liao, K. T. Wong, *J. Mater. Chem.* **2011**, 21, 9653-9660.
- [13] S. Tang, W.-Y. Tan, X.-H. Zhu, L. Edman, *Chem. Commun.* **2013**, 49, 4926-4928.
- [14] H. B. Wu, H. F. Chen, C. T. Liao, H. C. Su, K. T. Wong, *Org. Electron.* **2012**, 13, 483-490.
- [15] I.-S. Shin, H.-C. Lim, J.-W. Oh, J.-K. Lee, T. H. Kim, H. Kim, *Electrochemistry Communications* **2011**, 13, 64-67.
- [16] J. D. Slinker, A. A. Gorodetsky, M. S. Lowry, J. J. Wang, S. Parker, R. Rohl, S. Bernhard, G. G. Malliaras, *J. Am. Chem. Soc.* **2004**, 126, 2763-2767.

Figure Captions

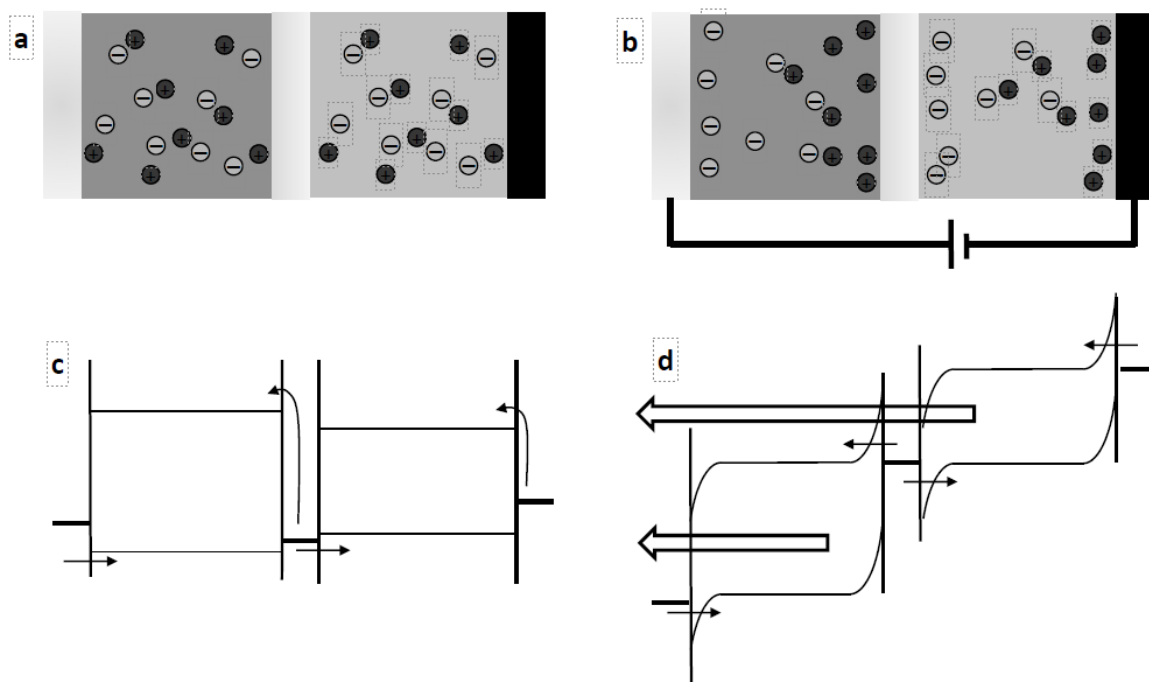


Figure 1. Operational mechanism of LECs and its application to a tandem configuration. (a) Schematic of a tandem LEC in which both the blue and orange light-emitting layers have ions. (b) Same tandem LEC as in panel (a) showing schematically the ion displacement when an external potential is applied. (c) Energy level diagram of the tandem LEC without external potential and (d) with external potential applied. The Fermi levels of the metals and the HOMO and LUMO levels of the blue and orange light-emitting materials are shown. The red solid arrows indicate large injection barriers for electron and holes, the green arrows indicate efficient electron and hole injection. The hollow arrows indicate the emission of light.

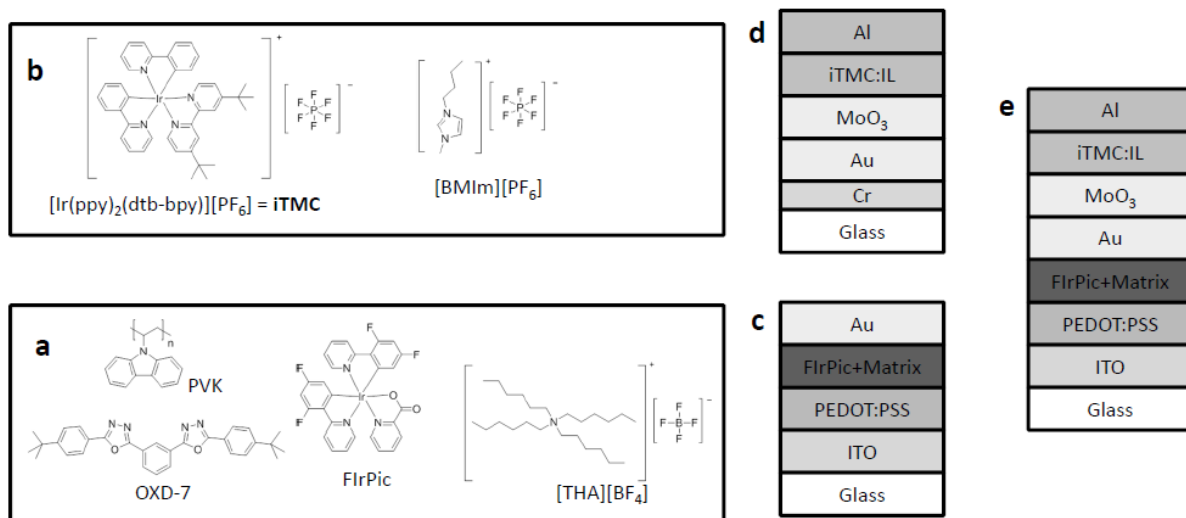


Figure 2. Structure of chemical compounds used and schematic of the device layouts. (a) Chemical structures of the compounds used for the bottom LEC. **(b)** Chemical structures of the compounds used for the top LEC. **(c)** Scheme of the bottom LEC layout. **(d)** Scheme of the top-LEC layout. **(e)** Scheme of the tandem-LEC layout.

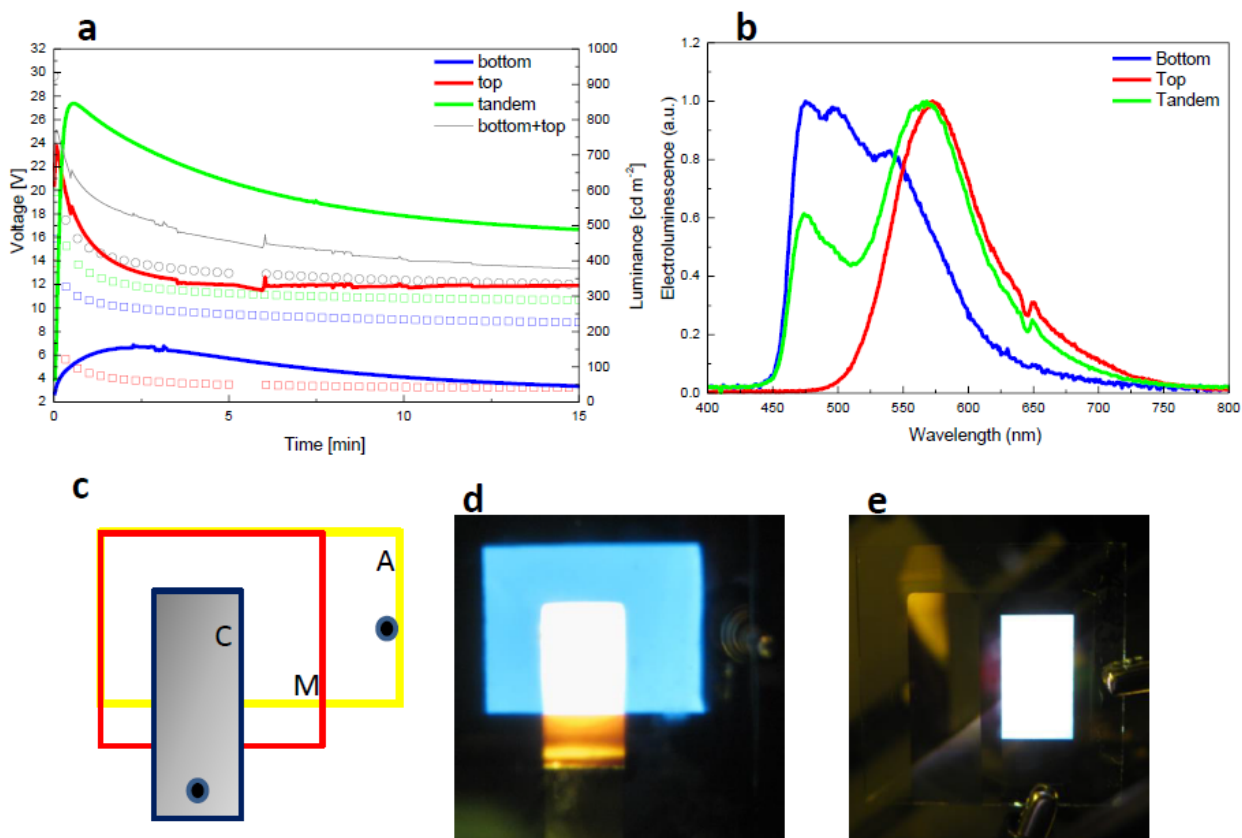


Figure 3. Performance of bottom-, top- and tandem-LECs. (a) Voltage (symbols) and luminance (lines) versus operation time for the bottom (blue), top (red), and tandem LECs (green) when operated at a constant current density of 100 A m^{-2} . (b) Electroluminescence spectra of the bottom (blue), top (red), and tandem LECs (green) when operated at a constant current density of 100 A m^{-2} . (c) Scheme depicting the position and size of the ITO bottom (A), Au middle (M), and Al top (C) electrodes, black dots indicate the position where the anode and cathode are contacted. (d) Photograph of a tandem LEC driven at 100 A m^{-2} with a 10 nm thick Au middle electrode. (e) Photograph of a tandem LEC driven at 100 A m^{-2} with a 5 nm thick Au middle electrode.

TOC

